Title

Clinical evaluation of white matter lesions on 3D inversion recovery ultrashort echo time MRI in multiple sclerosis

Journal

Quantitative Imaging in Medicine and Surgery, 0(0)

ISSN

2223-4292

Authors

Sedaghat, Sam

Jang, Hyungseok

Ma, Yajun

et al.

Publication Date

2023-07-01

DOI

10.21037/qims-22-1317

Peer reviewed

Original Article

Clinical evaluation of white matter lesions on 3D inversion recovery ultrashort echo time MRI in multiple sclerosis

Sam Sedaghat[1,2], Hyungseok Jang[1], Yajun Ma[1], Amir Masoud Afsahi[1], Benjamin Reichardt[3], Jody Corey-Bloom[4], Jiang Du[1,5,6]

[1]Department of Radiology, University of California, San Diego, CA, USA; [2]Department of Diagnostic and Interventional Radiology, University Hospital Heidelberg, Heidelberg, Germany; [3]Department of Interventional Radiology and Neuroradiology, Klinikum Hochsauerland, Arnsberg, Germany; [4]Department of Neurosciences, University of California, San Diego, CA, USA; [5]Department of Bioengineering, University of California, San Diego, CA, USA; [6]Radiology Service, Veterans Affairs San Diego Healthcare System, San Diego, CA, USA

Contributions: (I) Conception and design: S Sedaghat, H Jang, AM Afsahi, J Du; (II) Administrative support: S Sedaghat, H Jang, Y Ma, AM Afsahi, J Corey-Bloom, J Du; (III) Provision of study materials or patients: S Sedaghat, H Jang, Y Ma, J Corey-Bloom, J Du; (IV) Collection and assembly of data: S Sedaghat, H Jang, AM Afsahi, B Reichardt; (V) Data analysis and interpretation: S Sedaghat, H Jang, AM Afsahi, B Reichardt; (VI) Manuscript writing: All authors; (VII) Final approval of manuscript: All authors.

Correspondence to: Dr. Sam Sedaghat, MD. Department of Radiology, University of California San Diego (UCSD), 9500 Gilman Drive, CA 92093, USA. Email: samsedaghat1@gmail.com.

Background: We clinically evaluated the quality of white matter lesions (WML) of the cerebrum on 3D inversion recovery ultrashort echo time (IR-UTE) magnetic resonance imaging (MRI) in multiple sclerosis (MS) patients.

Methods: Forty-nine patients with MS were included in this study. A 3T MRI scanner was used. Two radiologists (readers) evaluated the quality of WML on IR-UTE images using a three-point Likert scale (1—good quality, 2—moderate quality, 3—insufficient quality). They also rated other WML-related factors potentially influencing WML quality using another three-point Likert scale (1—no/minor impact, 2—moderate impact, 3—high impact). Another reader rated the presence of WML on IR-UTE to evaluate the diagnostic value (right/false positive and false negative) of IR-UTE in detecting WML. Signal intensity ratios (SIRs) derived from WML signal intensities and WML sizes were also determined and analyzed.

Results: Two hundred and seventy-five MS lesions were evaluated. 87% of the lesions were rated Likert 1 on IR-UTE ($P<0.01$). WML rated Likert 2 and 3 presented near the grey matter (GM) in 58% of the cases (n=21), with 14 lesions being ≤2 mm ($P=0.03$). 62.5% of the WML rated Likert 2/3 were in the temporal lobe ($P=0.02$). The mean SIR of WML on IR-UTE was 1.14±0.22, while the mean SIR on fluid-attenuated inversion recovery (FLAIR) was 6.97±1.88. There was no significant correlation of SIRs between IR-UTE and FLAIR ($R=0.14$, $P=0.245$). 92.4% of the WML were correctly detected on IR-UTE (n=254). 19 out of the 21 false positive/negative rated WML were located near the GM or in the temporal lobe. WML presented 7.7% smaller in mean on IR-UTE compared to FLAIR. Factors affecting WML quality with a moderate or high impact (Likert 2 and 3) were not found.

Conclusions: Most WML are clearly detectable on IR-UTE sequences. The main limitations are WML in the temporal lobe and near the GM.

Keywords: Multiple sclerosis; magnetic resonance imaging (MRI); white matter; brain; diagnostics

Submitted Nov 27, 2022. Accepted for publication Mar 27, 2023. Published online May 04, 2023.
doi: 10.21037/qims-22-1317
View this article at: https://dx.doi.org/10.21037/qims-22-1317

Introduction

Multiple sclerosis (MS) is a chronic inflammatory disease causing severe disability to mainly young adults (1). The incidence and prevalence of MS are steadily increasing, with North America and Europe being the two most affected regions (2,3). MS usually presents two stages: an early relapsing-remitting disease and a delayed non-relapsing progression (1,4). Magnetic resonance imaging (MRI) is regarded to be of paramount importance for imaging in MS (5), as it comes along with high diagnostic performance in detecting MS lesions, monitoring disease progression, and evaluating treatment effects (6). MS lesions are assumed to show both the formation of new myelin sheaths around demyelinated axons (remyelination) and demyelination parallel within the same lesion (6,7).

In the routine clinical setting, different MRI sequences apply. T2-weighted (T2w) fluid-attenuated inversion recovery (FLAIR) and T1-weighted (T1w) images are mainly used for detecting white matter lesions (WML) in MS patients. However, conventional MRI sequences only provide qualitative imaging in MS (8), as T1w or T2w sequences only depict the longer T2 components in the WM that are not specific to myelin which has an extremely short T2 of less than 1 ms (9-18). With the introduction of ultrashort echo time (UTE)-type MRI sequences, the direct visualization of myelin protons within the white matter (WM) was enabled (9,15,16). Direct imaging of myelin protons is challenging because of its low proton density (thus low MR signal) and, among other things, rapid signal decay (13), requiring the use of minimum nominal TEs as short as 8 µs (17,18). That is much shorter than the TEs of conventional clinical sequences, typically in the order of several to tens of milliseconds (17). Additional adiabatic inversion recovery (IR) preparation allows uniform inversion and nulling of long T2 components with an appropriately chosen inversion time (TI). Short T2 components, presumably myelin, are saturated mainly by the long adiabatic inversion pulse due to its extremely fast transverse relaxation. As a result, the inversion recovery ultrashort echo time (IR-UTE) sequence allows direct and selective imaging of rapidly decaying myelin signal, which recovers during the TI and is detected by subsequent UTE data acquisition (9,13,17).

Although direct myelin imaging using IR-UTE is promising, previous publications solely focused on the feasibility of IR-UTE sequences or only depicted a few examples of lesions in MS. Consecutively, a systematic evaluation of WML quality on IR-UTE is not performed yet. However, a clinical evaluation is a requirement for possible later implementation in clinical practice. Therefore, our study aimed to evaluate the WML quality on IR-UTE. For this study, a 3D IR-UTE Cones sequence as one of the latest and most optimized IR-UTE sequences, was used. By adding a 3D Cones sampling to IR-UTE, the scan time can be reduced by more efficient k-space coverage (11,19).

Methods

Patients and image analysis

Forty-nine patients with MS were included in this study, which was reviewed and approved by the University of California San Diego Institutional Review Board (IRB). The study was conducted in accordance with the Declaration of Helsinki (as revised in 2013). Written informed consent approved by the IRB was obtained before each subject's participation. FLAIR and IR-UTE images were acquired from each subject. We performed three different analyses:

(I) Two readers rated the WML on IR-UTE images by determining the WML's quality using a manual segmentation. Three-point Likert scales were used for WML quality assessment with the following values: 1—good quality, 2—moderate quality, and 3—insufficient quality. Likert 1 was defined by a clear distinction of the WML from the adjacent normal-appearing white matter (NAWM). Likert 3 was defined as invisible or slightly hypointense WML. Likert 2 described a WML quality between Likert 1 and 3. The results and findings were reached by consensus. In this part of the study, WML on FLAIR images were set as the baseline. The readers also measured the sizes of WML on IR-UTE and FLAIR. Lesions in the grey matter (cortical lesions) were excluded, as they are not evaluable by the IR-UTE sequence. Also, infratentorial lesions were excluded due to the low signal-to-noise ratio (SNR). In the second step, the same readers evaluated other potential WML-related factors influencing WML quality: a confluence of WML, lobar WML distribution, hemispherical WML distribution, WML signal intensity, and the total number of WML. Here, another three-point Likert scale was used with the following values: 1—no/minor impact, 2—moderate impact, and 3—high impact. Additionally, the two readers measured the signal intensities (SIs) of the evaluated WML

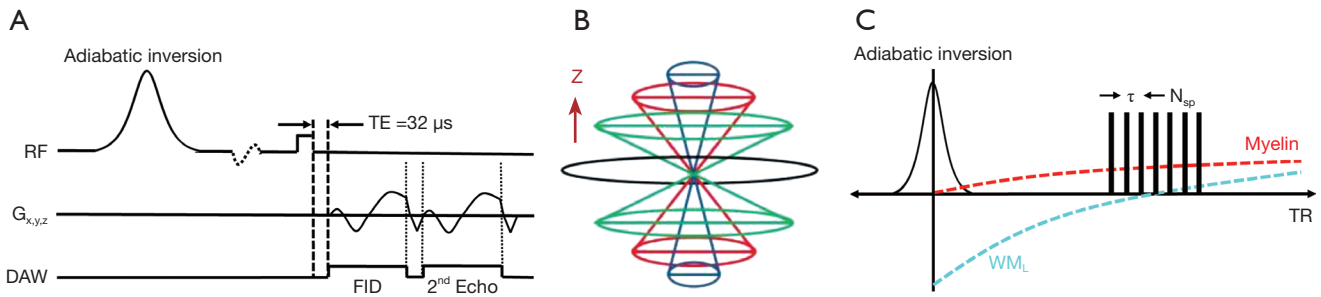

Figure 1 Principle of the 3D IR-UTE sequence for myelin imaging. (A) 3D IR-UTE sequence diagram, (B) the cones sampling strategy, (C) the myelin imaging contrast mechanism. The pulse sequence employs a long adiabatic inversion pulse to invert the longitudinal magnetization of WM_L, followed by a short rectangular pulse excitation and cones sampling with a minimal TE of 32 μs. The spiral trajectories are distributed along each cones for efficient sampling of the 3D k-space. The multi-spokes are sampled when the inverted longitudinal magnetization of WM_L approaches the nulling point. The residual long T2 signals are suppressed by subtracting the second echo from the first one, creating excellent contrast for myelin. IR-UTE, inversion recovery ultrashort echo time; WM_L, long T2 whiter matter; TE, echo time; DAW, data acquisition window; FID, free induction decay; Gx,y,z, gradient; N_{sp}, number of spokes; RF, radio frequency; TR, repetition time.

on IR-UTE and FLAIR images. From these SIs, SI ratios (SIRs) between SIs of the WML and the cerebrospinal fluid (CSF) were built.

(II) Another reader, who was blinded to the FLAIR images rated the presence of WML again on IR-UTE to evaluate the diagnostic value (right/false positive and false negative) of IR-UTE in detecting WML. Additionally, the reader measured the sizes of the identified WML on IR-UTE for the later comparison to the sizes of the same WML on FLAIR. The sizes of the corresponding FLAIR images were derived from the analyses performed before.

Images with stronger movement artifacts were excluded from the beginning (n=7 patients).

Lesion sizes were measured on the short axis.

3D IR-UTE Cones pulse sequence

A 3D IR-UTE Cones sequence was implemented on a 3 T whole-body scanner (MR750, GE Healthcare, Milwaukee, WI, USA). A 12-channel head coil was used for signal reception. The basic UTE sequence employs a short rectangular radiofrequency pulse for nonselective excitation in each acquisition, with a minimal nominal TE of 32 μs. Efficient sampling is achieved with a radial trajectory in the center of the k-space and a twisted spiral trajectory in the outer k-space. Spiral trajectories with conical ordering allow more efficient sampling of the 3D k-space (*Figure 1A*). The combination of 3D conical trajectories and multi-spoke acquisition further improves the time efficiency in volumetric imaging of short T2 components (11,19). Multiple acquisitions ("spokes") were applied after each IR preparation (11,20,21). A long Silver-Hoult adiabatic inversion pulse with a duration of 8.6 ms is used to uniformly invert the longitudinal magnetizations of long T2 water components in WM. With this pulse, water suppression only depends on the inversion time (TI), which is chosen to null the long T2 signals in WM (*Figure 1B*). The adiabatic inversion pulse also saturates the short T2 components, mainly myelin, which recover during the TI and are subsequently detected by multiple UTE acquisitions (11,20,22,23) (*Figure 1C*). A second echo is acquired to detect residual long T2 signals, with a near-zero signal for myelin because of its ultrafast signal decay. Finally, a dual-echo subtraction is performed to further reduce residual long T2 signals, providing selective myelin imaging (9,11). The remaining long T2 signal in WM will be suppressed, creating high-contrast imaging of myelin in WM (9,15,17,24). Against, in FLAIR, an inversion pulse is employed to invert and null fluid with a very long T1, leaving long T2 (but shorter T1) white matter and grey matter detected with high contrast.

MRI protocol

The MRI protocol included the following sequences:

Table 1 Quality [1-3] of WML not near the GM and non-temporal, WML near the GM and temporal lobe WML

Quality	WML (not near the GM and not associated with the temporal lobe)	WML near the GM	Temporal lobe WML	Total
1				239
≤2 mm	25	11	0	
>2 mm	165	32	6	
2				22
≤2 mm	2	9	3	
>2 mm	1	5	2	
3				14
≤2 mm	1	5	4	
>2 mm	1	2	1	

The data shows WML of ≤2 and >2 mm in size. WML, white matter lesion; GM, grey matter.

(I) the 3D IR-UTE Cones sequence a with a repetition time (TR) =1,000 ms, TI =320 ms, TE =0.032/2.2 ms, number of spokes (Nsp) =21, flip angle (FA) =20°, bandwidth =250 kHz, duration of each spoke () =7.1 ms, field of view (FOV) =22×22×15.1 cm^3, acquisition matrix =192×192×42, scan time =8.3 minutes; (II) a 3D T2-FLAIR sequence with TR =7,600 ms, TI =2,162 ms, TE =117 ms, FOV =25.6×25.6×25.6 cm^3, acquisition matrix =256×256×256, acceleration factor =4, scan time =6.9 minutes.

Statistical analysis

Baseline data are given as mean values with standard deviation (SD) or median with minimum and maximum. Distributions are indicated as percentages (%). Mann-Whitney-U-test and one-way ANOVA were performed to compare the group values. For comparing the three Likert groups to each other, the one-way ANOVA with a post-hoc Tukey test was performed. In all other cases, two groups were compared by using the Mann-Whitney-U-test. The WML quality groups (Likert 1–3) consisted of two or three groups, as indicated. Three-point Likert scales were also used for WML quality assessment and evaluation of impacting factors. SIRs of IR-UTE and FLAIR were correlated using Pearson's correlation "R". Statistical significance for all tests was set at P<0.05. Statistical analysis was done using the IBM-SPSS version 28.0 software package (IBM, Armonk, NY, USA).

Results

Baseline

The mean age of the patients was 58.6 years (SD: 11.8). 72% of the patients were female. The median EDSS of the patients was 3.5 (minimum: 2, maximum: 8). The mean time from the first examination at our institution to our MRI examination was 19.9 months (minimum: 9 months, maximum: 32 months). Two hundred and seventy-five WML were evaluated. 22% of the WML presented with a size of ≤2 mm, 35% of the WML with a size of >2 to <5 mm, and 43% of the WML were ≥5 mm.

WML quality and intensity on IR-UTE

Eighty seven percent of the WML were rated Likert 1 (good quality) on the UTE sequence (P<0.01; compared to Likert 2 and 3; ANOVA). 8% of the WML were rated Likert 2 (moderate quality) and 5% Likert 3 (insufficient quality) on the 3D IR-UTE sequence. *Table 1* presents an overview of the WML rating.

Figures 2,3 show examples of WML on IR-UTE and FLAIR images.

Within the WML, which were evaluated Likert 2 and 3, 58% presented near the GM (n=21), with 14 WML being ≤2 mm in diameter (P=0.03; compared to WML near the GM >2 mm; Mann-Whitney-U-test). 62.5% of the WML rated Likert 2 or 3 were in the temporal lobe (P=0.02;

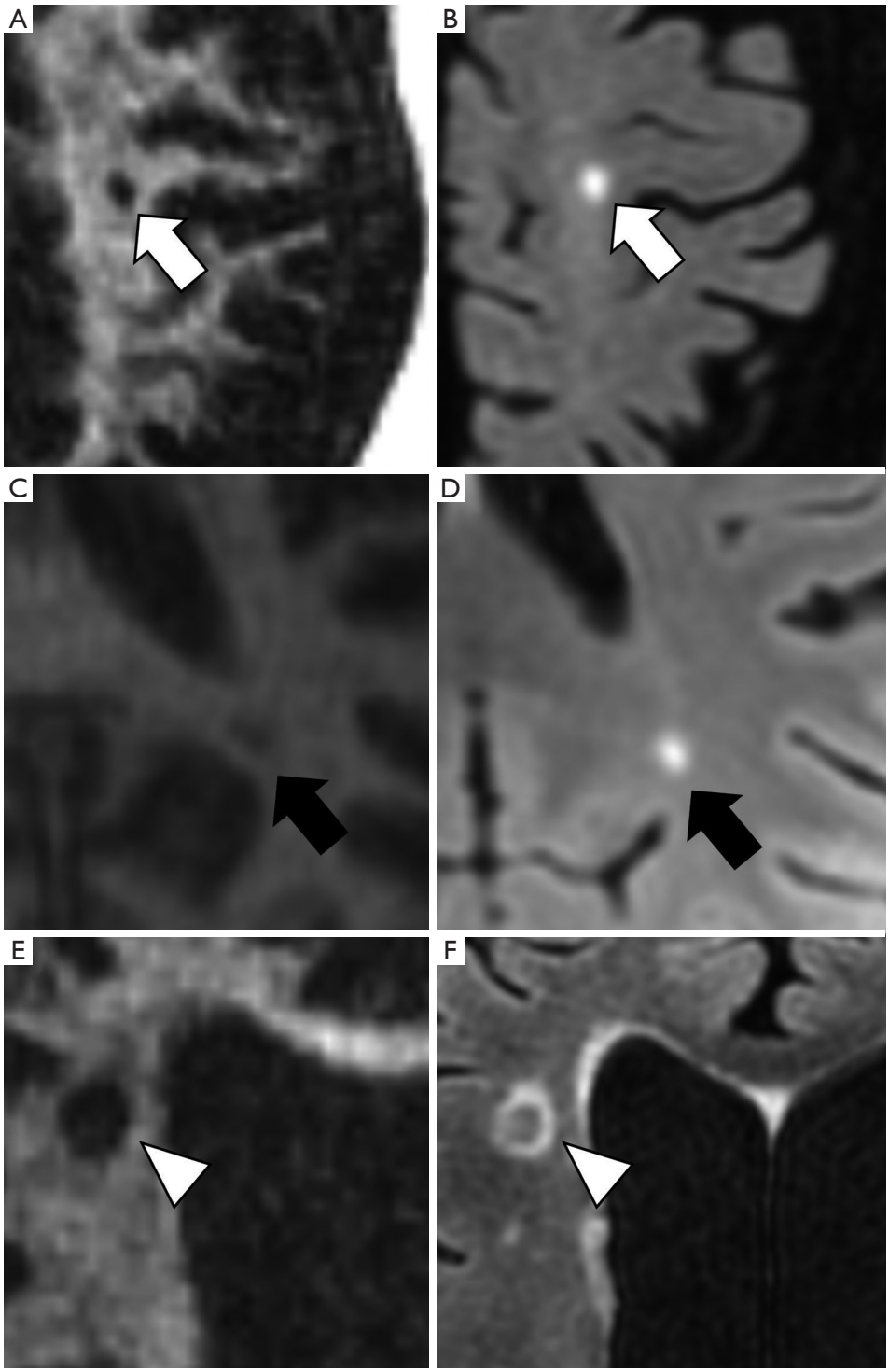

Figure 2 Examples of WML on 3D IR-UTE (A,C,E) and 3D FLAIR (B,D,F). (A,B) Show a lesion near the GM that is clearly to distinguish on both sequences (white arrow), while images (C,D) present a small lesion near the GM of under 2 mm (black arrow), which is not sufficient to detect on 3D IR-UTE. (E,F) Show a clearly identifiable periventricular WML (white arrowhead). WML, white matter lesion; IR-UTE, inversion recovery ultrashort echo time; FLAIR, fluid-attenuated inversion recovery; GM, grey matter.

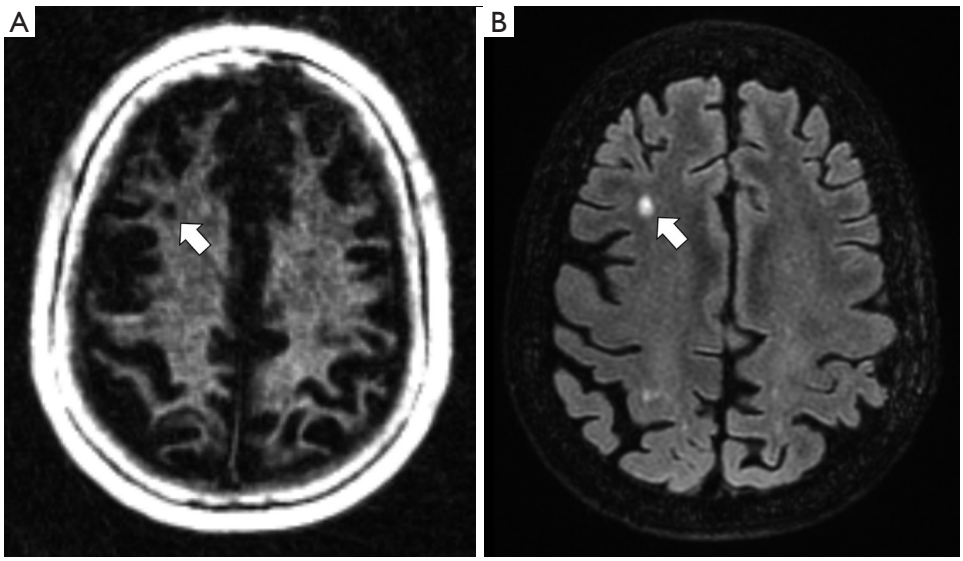

Figure 3 Whole brain image on 3D IR-UTE (A) and 3D FLAIR (B). A WML in the right frontal lobe is shown (white arrow). IR-UTE, inversion recovery ultrashort echo time; FLAIR, fluid-attenuated inversion recovery; WML, white matter lesion.

Table 2 Diagnostic performance of IR-UTE in detecting WML

Diagnostic parameters	n
True positive	254
False positive	5
False negative	16
Total	275

IR-UTE, inversion recovery ultrashort echo time; WML, white matter lesion.

compared to Likert 1 in the temporal lobe; Mann-Whitney-U-Test), with 7 being ≤2 mm. Against, 97% of the WML not near the GM and not associated with the temporal lobe were rated Likert 1 (P<0.01; compared to Likert 2 and 3; ANOVA).

The mean SIR of WMLs on IR-UTE was 1.14 (minimum: 0.74, maximum: 1.69, SD: 0.22), while the mean SIR on FLAIR was 6.97 (minimum: 2.5, maximum: 11.21, SD: 1.88). There was no significant correlation of SIRs between IR-UTE and FLAIR (R=0.14, P=0.245).

Diagnostic value of IR-UTE

92.4% of the WML were correctly detected on IR-UTE (n=254; *Table 2*). 1.8% of the WML were rated false positive (n=5) and 5.8% were false negative (n=16). 19 out of the 21 false positive/negative rated WML were located near the GM or in the temporal lobe.

Lesion sizes on IR-UTE compared to FLAIR

The mean WML size on IR-UTE was 4.67 mm (SD: 2.54 mm) and 5.08 mm (SD: 2.88 mm) on FLAIR. Overall, WML presented 7.7% smaller in mean on IR-UTE compared to FLAIR. The highest discrepancy was found in lesions <5 mm, where WML presented 9.4% smaller in mean on IR-UTE compared to FLAIR. In WML ≥5 mm, WML were 4.2% smaller in mean compared to FLAIR. The localization of the WML played no significant role in the deviation of sizes.

Further factors influencing WML quality

Eight patients presented multiple confluent lesions. The confluence of WML, WML distribution, the signal intensity of WML, and total numbers of WML had no/minor impact on the WML quality (Likert 1). WML-related factors leading to a moderate or high impact (Likert 2 or 3) could not be found.

Discussion

In this study, we evaluated the WML quality of the

cerebrum on IR-UTE MRI images in MS patients. As previous studies already showed the technical developments and feasibility of direct myelin imaging using UTE images (9-13,20), we focused on a clinical evaluation of this sequence by analyzing the WML quality.

One of the first steps taken after a patient is suspected of having MS is MRI because nearly all patients with multiple sclerosis present pathological MRI findings. With MRI, other findings unrelated to MS could also be identified or excluded, e.g., a leptomeningeal enhancement (25). Different MRI sequences, such as T1w and T2w images, are nowadays routinely used in clinics and are mandatory for the radiological evaluation of the disease (26). In some cases, post-contrast T1w sequences are added (25,27,28).

UTE MRI sequences have 100–1,000 times shorter echo times than conventional sequences (9,12,15-17,29-32), which allows selective and direct imaging of myelin protons (9,11,33). What is visualized with UTE sequences mainly represents myelin lipids (13). Also, histopathological studies revealed that the distribution of short-T2 components correlates with the presence of myelin (17). Accordingly, the absence of short T2 is associated with the absence of myelin in MS plaques (8).

In our study, we excluded cortical and infratentorial lesions. Cortical lesions in the grey matter have a much lower myelin density than the WM (34,35), while infratentorial lesions typically show a low SNR on IR-UTE. Therefore, IR-UTE provides some limitations for grey matter and infratentorial imaging, making it more challenging to distinguish MS lesions in these regions on IR-UTE.

We propose a field strength of 3T for clinical use, as most previous studies suggested the same field strength (9,11,17,36). The suitable TI choice is also critical to minimizing water contamination (12,37), which should lie around 320 ms.

Our study shows that most WML are clearly seen on IR-UTE images, which is a requirement for a possible implementation of IR-UTE sequences in the routine clinical setting at a later stage. Also, 92.4% of the WML were correctly detected on IR-UTE compared to FLAIR. The main limitations are in WML near the GM and the temporal lobe. As an explanation, these regions are nearer to the grey matter, which is typically challenging for UTE. Another issue is smaller WML, which are often underestimated in size on IR-UTE.

IR-UTE sequences should not be regarded as a substitute for FLAIR images but as a supplemental sequence. As described by previous studies, an advantage of IR-UTE could lie in direct myelin imaging, which allows direct quantification of myelin and myelin mapping (9,12,17,31,32,38). However, reliable WML-specific mapping methods using IR-UTE have not been published yet. Our study also did not investigate myelin mapping techniques or sophisticated quantitative analysis of WML on IR-UTE. Nevertheless, we compared the SIs of WML on IR-UTE and FLAIR and found no significant correlation. This finding is reasonable, as direct myelin imaging using UTE has the potential to directly visualize components and processes within WML compared to FLAIR. Future studies should focus on a combined approach using qualitative and quantitative techniques for evaluating WML on IR-UTE to improve diagnostics and treatment monitoring (e.g., remyelination therapy) (39) of MS and other neurological diseases.

There are still some improvements necessary to allow broad use of IR-UTE in the routine clinical setting. Therefore, future studies should also focus on optimizing IR-UTE for clinical use and developing automated qualitative and quantitative UTE-based analyses of WML. Especially an automated approach using direct myelin imaging would accelerate the implementation of IR-UTE sequences into the routine clinical setting, as physicians will not have the time to perform sophisticated quantitative analyses manually.

Several limitations to our study exist. First, the 3D IR-UTE sequence is relatively slow, with a total scan time of 8.3 minutes. Head motion was observed in some patients, leading to degraded image quality. More advanced data acquisition and reconstruction techniques are needed to reduce the total scan time for improved clinical performance. Second, MS lesions investigated in our study could not be examined histologically. Lesions on the FLAIR images are used as the reference standard. Third, selective myelin imaging highly depends on water suppression. Imperfect suppression of long T2 WM components may result in water contamination, which has minimal effect on morphological imaging but may significantly affect quantitative myelin imaging, such as myelin density quantification (17). Fourth, myelin imaging is subject to low signal due to its inherently fast signal decay and relatively low proton density. Relatively low spatial resolution is used in myelin imaging to partly compensate for this limitation, leading to potential partial volume artifacts. Nevertheless,

with 3D sequences, partial volume artifacts, which are a potential source of error, are reduced (17). Finally, we did not investigate cortical and juxtacortical lesions, as this approach is more challenging due to the lower density of myelin protons (17). More advanced techniques are needed for high-contrast myelin imaging in GM and GM-near lesions.

Conclusions

Most WML are clearly identified on 3D IR-UTE images. Nevertheless, WML near the GM or in the temporal lobe poses a limitation on 3D IR-UTE, especially when the WML is ≤2 mm in size. Further optimizations of this sequence should focus on an optimized visualization of GM lesions and WML near the GM. Direct myelin imaging using IR-UTE could become a promising supplemental sequence for WML diagnostics in MS patients.

Acknowledgments

Funding: The authors acknowledge grant support from the Deutsche Forschungsgemeinschaft (No. SE 3272/1-1), the National Institutes of Health (Nos. RF1AG075717 and R01NS092650), the VA Clinical Science Research & Development Service (No. I01CX002211), and GE Healthcare.

Footnote

Conflicts of Interest: All authors have completed the ICMJE uniform disclosure form (available at https://qims.amegroups.com/article/view/10.21037/qims-22-1317/coif). JD serves as an unpaid editorial board member of *Quantitative Imaging in Medicine and Surgery*. The other authors have no conflicts of interest to declare.

Ethical Statement: The authors are accountable for all aspects of the work in ensuring that questions related to the accuracy or integrity of any part of the work are appropriately investigated and resolved. This study was approved by the Institutional Review Board (IRB) of the University of California San Diego. The study was conducted in accordance with the Declaration of Helsinki (as revised in 2013). Written informed consent approved by the IRB was obtained before each subject's participation.

References

1. Dobson R, Giovannoni G. Multiple sclerosis - a review. Eur J Neurol 2019;26:27-40.
2. Browne P, Chandraratna D, Angood C, Tremlett H, Baker C, Taylor BV, Thompson AJ. Atlas of Multiple Sclerosis 2013: A growing global problem with widespread inequity. Neurology 2014;83:1022-4.
3. Oh J, Vidal-Jordana A, Montalban X. Multiple sclerosis: clinical aspects. Curr Opin Neurol 2018;31:752-9.
4. Leray E, Yaouanq J, Le Page E, Coustans M, Laplaud D, Oger J, Edan G. Evidence for a two-stage disability progression in multiple sclerosis. Brain 2010;133:1900-13.
5. Inglese M, Petracca M. MRI in multiple sclerosis: clinical and research update. Curr Opin Neurol 2018;31:249-55.
6. Filippi M, Brück W, Chard D, Fazekas F, Geurts JJG, Enzinger C, Hametner S, Kuhlmann T, Preziosa P, Rovira À, Schmierer K, Stadelmann C, Rocca MA; . Association between pathological and MRI findings in multiple sclerosis. Lancet Neurol 2019;18:198-210.
7. Miron VE, Franklin RJ. Macrophages and CNS remyelination. J Neurochem 2014;130:165-71.
8. Laule C, Moore GRW. Myelin water imaging to detect demyelination and remyelination and its validation in pathology. Brain Pathol 2018;28:750-64.
9. Du J, Ma G, Li S, Carl M, Szeverenyi NM, VandenBerg S, Corey-Bloom J, Bydder GM. Ultrashort echo time (UTE) magnetic resonance imaging of the short T2 components in white matter of the brain using a clinical 3T scanner. Neuroimage 2014;87:32-41.
10. Du J, Bydder GM. Qualitative and quantitative ultrashort-TE MRI of cortical bone. NMR Biomed 2013;26:489-506.
11. Ma YJ, Searleman AC, Jang H, Fan SJ, Wong J, Xue Y, Cai Z, Chang EY, Corey-Bloom J, Du J. Volumetric imaging of myelin in vivo using 3D inversion recovery-prepared ultrashort echo time cones magnetic resonance imaging. NMR Biomed 2020;33:e4326.
12. Ma YJ, Jang H, Chang EY, Hiniker A, Head BP, Lee RR, Corey-Bloom J, Bydder GM, Du J. Ultrashort echo time

(UTE) magnetic resonance imaging of myelin: technical developments and challenges. Quant Imaging Med Surg 2020;10:1186-203.
13. Jang H, Ma Y, Searleman AC, Carl M, Corey-Bloom J, Chang EY, Du J. Inversion recovery UTE based volumetric myelin imaging in human brain using interleaved hybrid encoding. Magn Reson Med 2020;83:950-61.
14. Soustelle L, Antal MC, Lamy J, Rousseau F, Armspach JP, Loureiro de Sousa P. Correlations of quantitative MRI metrics with myelin basic protein (MBP) staining in a murine model of demyelination. NMR Biomed 2019;32:e4116.
15. Horch RA, Gore JC, Does MD. Origins of the ultrashort-T2 1H NMR signals in myelinated nerve: a direct measure of myelin content? Magn Reson Med 2011;66:24-31.
16. Wilhelm MJ, Ong HH, Wehrli SL, Li C, Tsai PH, Hackney DB, Wehrli FW. Direct magnetic resonance detection of myelin and prospects for quantitative imaging of myelin density. Proc Natl Acad Sci U S A 2012;109:9605-10.
17. Sheth V, Shao H, Chen J, Vandenberg S, Corey-Bloom J, Bydder GM, Du J. Magnetic resonance imaging of myelin using ultrashort Echo time (UTE) pulse sequences: Phantom, specimen, volunteer and multiple sclerosis patient studies. Neuroimage 2016;136:37-44.
18. Boucneau T, Cao P, Tang S, Han M, Xu D, Henry RG, Larson PEZ. In vivo characterization of brain ultrashort-T(2) components. Magn Reson Med 2018;80:726-35.
19. Gurney PT, Hargreaves BA, Nishimura DG. Design and analysis of a practical 3D cones trajectory. Magn Reson Med 2006;55:575-82.
20. Ma YJ, Zhu Y, Lu X, Carl M, Chang EY, Du J. Short T(2) imaging using a 3D double adiabatic inversion recovery prepared ultrashort echo time cones (3D DIR-UTE-Cones) sequence. Magn Reson Med 2018;79:2555-63.
21. Carl M, Bydder GM, Du J. UTE imaging with simultaneous water and fat signal suppression using a time-efficient multispoke inversion recovery pulse sequence. Magn Reson Med 2016;76:577-82.
22. Larson PE, Conolly SM, Pauly JM, Nishimura DG. Using adiabatic inversion pulses for long-T2 suppression in ultrashort echo time (UTE) imaging. Magn Reson Med 2007;58:952-61.
23. Manhard MK, Horch RA, Harkins KD, Gochberg DF, Nyman JS, Does MD. Validation of quantitative bound- and pore-water imaging in cortical bone. Magn Reson Med 2014;71:2166-71.
24. Fan SJ, Ma Y, Chang EY, Bydder GM, Du J. Inversion recovery ultrashort echo time imaging of ultrashort T(2) tissue components in ovine brain at 3 T: a sequential D(2) O exchange study. NMR Biomed 2017.
25. Brownlee WJ, Hardy TA, Fazekas F, Miller DH. Diagnosis of multiple sclerosis: progress and challenges. Lancet 2017;389:1336-46.
26. Filippi M, Rocca MA, Ciccarelli O, De Stefano N, Evangelou N, Kappos L, Rovira A, Sastre-Garriga J, Tintorè M, Frederiksen JL, Gasperini C, Palace J, Reich DS, Banwell B, Montalban X, Barkhof F; . MRI criteria for the diagnosis of multiple sclerosis: MAGNIMS consensus guidelines. Lancet Neurol 2016;15:292-303.
27. Rovira À, Wattjes MP, Tintoré M, Tur C, Yousry TA, Sormani MP, De Stefano N, Filippi M, Auger C, Rocca MA, Barkhof F, Fazekas F, Kappos L, Polman C, Miller D, Montalban X; . Evidence-based guidelines: MAGNIMS consensus guidelines on the use of MRI in multiple sclerosis-clinical implementation in the diagnostic process. Nat Rev Neurol 2015;11:471-82.
28. Matthews PM. Chronic inflammation in multiple sclerosis - seeing what was always there. Nat Rev Neurol 2019;15:582-93.
29. Ma YJ, Searleman AC, Jang H, Wong J, Chang EY, Corey-Bloom J, Bydder GM, Du J. Whole-Brain Myelin Imaging Using 3D Double-Echo Sliding Inversion Recovery Ultrashort Echo Time (DESIRE UTE) MRI. Radiology 2020;294:362-74.
30. Jang H, Ma YJ, Chang EY, Fazeli S, Lee RR, Lombardi AF, Bydder GM, Corey-Bloom J, Du J. Inversion Recovery Ultrashort TE MR Imaging of Myelin is Significantly Correlated with Disability in Patients with Multiple Sclerosis. AJNR Am J Neuroradiol 2021;42:868-74.
31. Du J, Sheth V, He Q, Carl M, Chen J, Corey-Bloom J, Bydder GM. Measurement of T1 of the ultrashort T2* components in white matter of the brain at 3T. PLoS One 2014;9:e103296.
32. Ma YJ, Jang H, Wei Z, Wu M, Chang EY, Corey-Bloom J, Bydder GM, Du J. Brain ultrashort T(2) component imaging using a short TR adiabatic inversion recovery prepared dual-echo ultrashort TE sequence with complex echo subtraction (STAIR-dUTE-ES). J Magn Reson 2021;323:106898.
33. Seifert AC, Li C, Wilhelm MJ, Wehrli SL, Wehrli FW. Towards quantification of myelin by solid-state MRI of the lipid matrix protons. Neuroimage 2017;163:358-67.
34. Uddin MN, Figley TD, Solar KG, Shatil AS, Figley CR.

Comparisons between multi-component myelin water fraction, T1w/T2w ratio, and diffusion tensor imaging measures in healthy human brain structures. Sci Rep 2019;9:2500.
35. Norton WT, Cammer W. Isolation and characterization of myelin. In: Myelin. Springer, 1984:147-95.
36. He Q, Ma Y, Fan S, Shao H, Sheth V, Bydder GM, Du J. Direct magnitude and phase imaging of myelin using ultrashort echo time (UTE) pulse sequences: A feasibility study. Magn Reson Imaging 2017;39:194-9.
37. Carl M, Koch K, Du J. MR imaging near metal with undersampled 3D radial UTE-MAVRIC sequences. Magn Reson Med 2013;69:27-36.
38. Ma YJ, Jang H, Wei Z, Cai Z, Xue Y, Lee RR, Chang EY, Bydder GM, Corey-Bloom J, Du J. Myelin Imaging in Human Brain Using a Short Repetition Time Adiabatic Inversion Recovery Prepared Ultrashort Echo Time (STAIR-UTE) MRI Sequence in Multiple Sclerosis. Radiology 2020;297:392-404.
39. Cunniffe N, Coles A. Promoting remyelination in multiple sclerosis. J Neurol 2021;268:30-44.

Cite this article as: Sedaghat S, Jang H, Ma Y, Afsahi AM, Reichardt B, Corey-Bloom J, Du J. Clinical evaluation of white matter lesions on 3D inversion recovery ultrashort echo time MRI in multiple sclerosis. Quant Imaging Med Surg 2023;13(7):4171-4180. doi: 10.21037/qims-22-1317

